Clim Dyn (2015) 45:3481–3492
DOI 10.1007/s00382-015-2551-z

Connection between weak stratospheric vortex events and the Pacific Decadal Oscillation

Sung-Ho Woo[1] · Mi-Kyung Sung[2] · Seok-Woo Son[3] · Jong-Seong Kug[1]

Received: 30 June 2014 / Accepted: 2 March 2015 / Published online: 12 March 2015
© Springer-Verlag Berlin Heidelberg 2015

Abstract We investigate the possible impacts of the Pacific Decadal Oscillation (PDO) on the occurrence of weak stratospheric polar vortex (WSV) events in the Northern Hemisphere winter. WSV events, which are defined when polar-cap geopotential height anomalies at 50 hPa fall below the 10th percentile in winter, are observed more frequently during positive PDO phases than during negative PDO phases. Additionally, tropospheric wave forcings that drive WSV events are remarkably different between the two phases of the PDO. During the positive PDO phase, the vertical propagation of wavenumber-one waves plays a predominant role with a rather minor contribution of wavenumber-two waves. This contrasts with the negative PDO phase when the WSV events are primarily caused by wavenumber-two waves. This difference is partly related to the PDO-induced tropospheric circulation anomalies over the North Pacific whose zonal wavenumber-one component constructively (destructively) interferes with climatological planetary-scale waves during positive (negative) PDO winters. The predominant wavenumber-two wave forcings during the negative PDO phase are likely related to the enhanced tropospheric eddy activity over Alaska that results from the poleward shift of the Pacific jet in response to the negative PDO.

✉ Jong-Seong Kug
jskug@postech.ac.kr

[1] School of Environmental Science and Engineering, Pohang University of Science and Technology (POSTECH), Pohang, Gyungbuk 790-784, South Korea

[2] Division of Climate Change, Korea Polar Research Institute, Incheon, South Korea

[3] School of Earth and Environmental Sciences, Seoul National University, Seoul, South Korea

Keywords PDO · Weak stratospheric vortex events · Troposphere–stratosphere interaction

1 Introduction

The variability of the stratospheric polar vortex dominates the intraseasonal variability of the stratospheric circulation in the Northern Hemisphere winter (Andrews et al. 1987). In particular, the breakdown or abrupt weakening of the polar vortex, which is often referred to as the stratospheric sudden warming (SSW; Matsuno 1971) or weak stratospheric vortex (WSV; Baldwin and Dunkerton 2001) event (see Butler et al. 2015 for various definitions of such events), accompanies the rise of stratospheric temperatures and geopotential heights (Z) over the polar region. The impact of the event is not confined to the stratosphere but extends to the surface on a time scale of a few weeks. The resulting surface anomalies often resemble the negative phase of the Arctic Oscillation (Hartley et al. 1998; Baldwin and Dunkerton 1999, 2001; Thompson et al. 2002; Limpasuvan et al. 2004; Perlwitz and Harnik 2004; Black 2002; Charlton et al. 2007; Mitchell et al. 2013), which majorly influences the regional weather and climate systems (Thompson et al. 2002; Yun et al. 2014).

This coupling between the stratosphere and troposphere suggests that the stratospheric variability has the potential to improve extended weather and seasonal predictions. This possibility has been actively explored in the most recent decade (e.g., Stan and Straus 2009; Sigmond et al. 2013), and most operational models now have a model top at or above the stratopause (e.g., Charron et al. 2012; see also the recent reviews by Gerber et al. (2012) and Tripathi et al. (2014)). Therefore, a better understanding of the polar vortex variability and related dynamics, particularly

those associated with WSV events, is valuable for advancing our scientific knowledge and for improving operational forecasts.

WSV events are mainly driven by zonal wavenumber-one or wavenumber-two (hereafter W1 and W2, respectively) waves that propagate from the upper troposphere to the stratosphere (Matsuno 1970; Andrews et al. 1987; Kim et al. 2014). As a simple approach to identify the tropospheric precursors of WSV events, a linear framework has been recently proposed (Nishii et al. 2009; Garfinkel et al. 2010; Smith et al. 2010). It is suggested that tropospheric anomalies that influence the stratospheric polar vortex can be partly understood by considering the linear interference between the climatological waves and the regional circulation anomalies. For example, a positive Z anomaly over Northern Europe tends to constructively interfere with the climatological W2 component in the troposphere, resulting in enhanced W2-wave propagation into the stratosphere. Likewise, a negative Z anomaly over the North Pacific tends to strengthen the upward propagation of W1 waves (Garfinkel et al. 2010). In addition, the authors noted that a positive Z anomaly over the northeastern Pacific can strengthen W2 waves. This difference in wave forcings can result in different types of WSV events, such as displacement or split types (e.g., Charlton et al. 2007; Martius et al. 2009). Mitchell et al. (2013) suggested that the different types of WSV events may have different surface impacts; they showed that a vortex-split event is more robustly related to surface anomalies than a displacement event. Although this result is subject to the definition and detection algorithm of WSV events (for instance, Charlton et al. (2007) found insensitive differences in the surface responses to the two types of SSW events), it is important to understand the sources of tropospheric precursors that determine the characteristics of WSV events.

A number of studies have been conducted on the possible sources of tropospheric wave activity that affects the polar vortex. As a remote boundary forcing, tropical sea surface temperature (SST) anomalies, particularly those associated with the El Niño-Southern Oscillation (ENSO), have been proposed to modulate the seasonal-mean state of the winter stratosphere through the Pacific/North American teleconnection (PNA) pattern and the resulting vertical propagation of planetary-scale waves in the extratropics (Manzini et al. 2006; Taguchi and Hartmann 2006; Garfinkel and Hartmann 2007). In particular, during an El Niño winter, the seasonal-mean polar vortex tends to be weaker (and warmer) than normal (Bronnimann 2007; Garfinkel and Hartmann 2007; Bell et al. 2009). Opposite stratospheric anomalies are observed during La Niña winters, but the signal is weaker than that during the El Niño state (Sassi et al. 2004; Manzini et al. 2006; Garfinkel and Hartmann 2007; Free and Seidel 2009). Butler and Polvani (2011), however, found no evidence of a frequency change of SSW events during the two phases of the ENSO. As a possible culprit, Garfinkel et al. (2012) suggested that the extreme negative Z anomaly in the northwest region of the Bering Sea, which is reported as one of the WSV precursor regions, shows similar frequency between both phases of the ENSO.

In addition to the tropical SST forcing, recent studies have documented a potential impact of extratropical SST anomalies in the North Pacific on stratospheric circulation changes. Taguchi et al. (2012) noted that the seasonal evolution of PNA-like Z anomalies may develop as a response to the persistent SST anomalies over the North Pacific frontal zone. Likewise, Lee et al. (2012) suggested that the PDO can contribute to Pacific storm-track changes by altering the lower-tropospheric temperature field. These anomalies are able to generate vertically propagating planetary-scale waves in the stratosphere, potentially affecting the characteristics of WSV events. In fact, Jadin et al. (2010) showed that the vertical propagation of planetary-scale waves is somewhat modulated by the PDO-related SST anomalies over the North Pacific in early winter. By integrating AGCM with prescribed North Pacific SST anomalies, Hurwitz et al. (2012) further confirmed this finding. The authors showed that North Pacific SST anomalies can modify planetary-scale wave activity in the stratosphere, affecting the frequency of SSW events. The frequency of SSW events substantially increases when cold SSTs are prescribed in the North Pacific in model simulations.

These studies suggest that not only tropical but also extratropical SST anomalies are able to modulate planetary-scale wave activity in the wintertime stratosphere. The latter anomalies can be directly related to PDO, as reported by Jadin et al. (2010). However, a dynamical link between the PDO and stratospheric circulation anomalies has not been well established in the observations. For instance, it remains unclear how the PDO affects the frequency and morphology of WSV events. By analyzing long-term reanalysis data, the present study documents the observed relationship between the PDO and WSV events. The possible dynamical processes are also briefly discussed.

After describing the data in the next section, the WSV events are defined and general features of the detected events are introduced. Then, tropospheric precursors of WSV events during the two PDO phases and the related dynamical processes are discussed. Finally, the overall findings are briefly summarized.

2 Data and method

The National Centers for Environmental Prediction/National Center for Atmospheric Research (NCEP/NCAR)

reanalysis data, which provides long-term daily data up to 10 hPa (Kalnay et al. 1996), are used in this study to increase the sample size of the WSV events. Specifically, a total of 63 winters (December to March) from 1948/1949 to 2010/2011 are analyzed in a standard resolution of 2.5° longitude by 2.5° latitude. The daily anomaly field is obtained by removing the smoothed (21-day running mean) daily climatology from the raw data. In addition, to examine the precondition features of WSV events according to PDO phases, composite analysis is mainly used. The statistical significance is computed based on a two-tailed Student's t test.

2.1 Pacific Decadal Oscillation (PDO) index

The seasonal-mean PDO index, which is defined as the leading principal component of the sea surface temperature (SST) anomalies over the Pacific Ocean, north of 20°N (available at http://jisao.washington.edu/pdo/PDO.latest), is used in this study. The resulting time series, normalized by its standard deviation, is presented in Fig. 1. As documented in the literature, the PDO index has changed its sign from the negative in the 1950s and 1960s to the positive in the 1980s, and negative again in the late 2000s. In addition to this decadal variability, there is significant year-to-year variability.

2.2 Weak stratospheric vortex (WSV) events

The variability of the stratospheric polar vortex has often been evaluated using the Northern Annular Mode (NAM) index (e.g., Baldwin and Dunkerton 2001) or polar-cap geopotential height anomaly integrated over 65°–90°N (e.g., Cohen et al. 2002; Kolstad et al. 2010; Martineau and Son 2013). The latter measure is essentially the same as the canonical NAM index, with a significant negative correlation (e.g., Baldwin and Thompson 2009). Following Kolstad et al. (2010), the latter measure, the polar-cap geopotential height anomalies (hereafter "Z_p anomaly" for brevity), is used to detect WSV events. Specifically, the onset of the event is defined as the 1st day when the $-Z_p$ anomaly at 50 hPa is lower than the 10th percentile (−292.4 m). Here, the negative sign reflects the negative correlation between the zonal wind and polar-cap Z anomalies during WSV events. The last day is defined as the end of a continuous period of $-Z_p$ anomalies lower than the −0.5 standard deviation at 100 hPa. If there is another onset day during the life cycle of individual WSV events, then we consider the two events a single WSV event. Based on this approach, a total of 48 WSV events are identified. This number corresponds to about 0.78 events per winter, which is a slightly higher frequency than that of major SSW events identified by the WMO definition (Andrews et al. 1987; see also Fig. 2 of Butler et al. 2015). Not surprisingly, more than 70 % of the WSV events analyzed in this study are classified as major SSW events, and the overall results are not sensitive to the definition.

The WSV events are grouped into two categories according to the PDO phase, i.e., WSV events during the positive PDO phase (+PWSV events) and those during the negative phase (−PWSV events); these events are selected when the PDO index is larger than its 0.5 standard deviation or smaller than its −0.5 standard deviation, respectively. A total of 19 +PWSV (0.83 events per positive PDO winter) and 13 −PWSV events (0.62 events per negative PDO winter) are detected, with 16 WSV events during the neutral PDO state (0.80 events per neutral PDO winter). The frequency of −PWSV events is lower than that of +PWSV events. To examine whether the frequency of +PWSV events is significantly different from it of −PWSV events, the significance test based on bootstrap method is performed. Firstly, we randomly select 19 (13) years for 23 positive (21 negative) PDO years, and calculate frequency of WSV events during the selected years in each PDO phase. These processes are repeated in 10,000 times. Then, we obtain a probability density function of frequency for WSV events in two PDO phases. Based on these statistics, we found that the difference in the frequencies of WSV events between both PDO phases is statistically significant. More importantly, this result is qualitatively consistent with the modeling study of Hurwitz et al. (2012), which showed a more frequent occurrence of WSV events when cold SSTs are prescribed over the North Pacific. Because of the decadal nature of the PDO, −PWSV events primarily occurred before the 1980s, whereas +PWSV events occurred afterward, as indicated in Fig. 1.

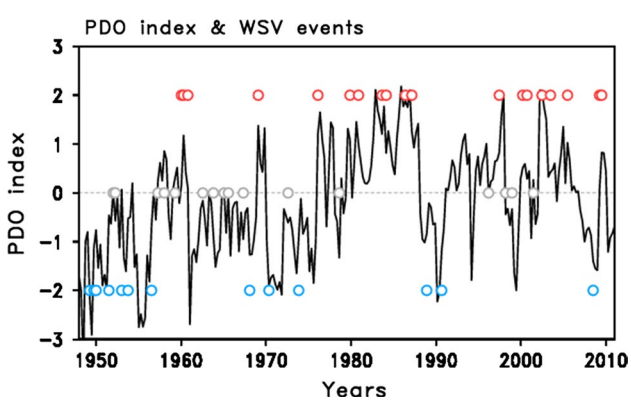

Fig. 1 The monthly PDO index time series and WSV events. The *red*, *blue* and *gray circles* indicate that the WSV event occurred during positive, negative and neutral PDO phases, respectively. The markers for the WSV events are arbitrarily placed at +2, 0 and −2 for positive, negative and neutral PDO phases, respectively

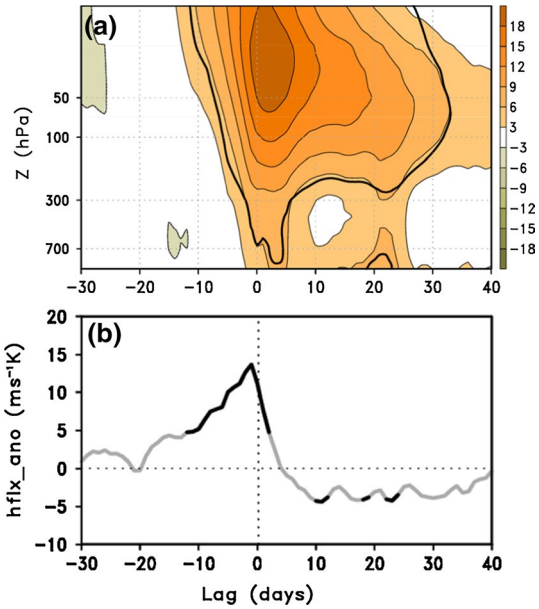

Fig. 2 **a** Lag composite of the normalized Z anomalies averaged over 65°N northward and **b** the zonal-mean meridional heat flux averaged over 40°–70°N at 100 hPa before and after the onset of the WSV event (lag 0). The area inside the *thick black line* in **a** and the *thick black lines* in **b** satisfies the 95 % confidence level

3 Results

To verify the detection of WSV events, we first investigate the temporal evolution of polar-cap Z anomalies during the WSV events. Figure 2a shows the lead-lag composite of the Z_p anomalies as a function of pressure and time. The positive anomalies are prominent in the stratosphere for more than a month; they start to develop at a lag of −10 days and reach the maximum value at a lag of 3 days. After the peak, the positive anomalies slowly decay over time. Most of these anomalies are statistically significant at the 95 % confidence level. Figure 2a further shows significant anomalies near the surface around lags of 0 and 20 days, which are coupled to the stratospheric anomalies. These features, the persistence of stratospheric anomalies and the downward coupling to the troposphere, are well documented in the literature (e.g., Baldwin and Dunkerton 2001; Charlton et al. 2007).

Figure 2b illustrates the evolution of the poleward eddy heat flux anomaly at 100 hPa integrated over 40°–70°N. This quantity, which is proportional to the vertical component of the Eliassen-Palm flux in quasi-geostrophic linear-wave dynamics (e.g., Andrews et al. 1987), is widely used in the literature to evaluate upward propagating waves from the upper troposphere to the stratosphere (e.g., Polvani and Waugh 2004). A positive anomaly appears in the negative time lags, indicating the growth of upward-propagating waves before the onset of the WSV events. The waves gradually strengthen from a lag of −20 to −1 days and then rapidly decay in a few days. This upward-propagating wave change is consistent with previous studies (e.g., see Fig. 4 of Polvani and Waugh 2004). Because Fig. 2b shows a statistically significant eddy heat flux from a lag of −11 to −1 days, in the next section, we examine precursor patterns of the WSV events during this preconditioning period.

3.1 Tropospheric preconditioning of WSV events

As mentioned earlier, the variability of the stratospheric polar vortex is largely determined by upward-propagating planetary-scale waves. Such waves are significantly modulated by the anomalous circulation over northern Europe and the North Pacific (Garfinkel et al. 2010; Kolstad and Charlton-Perez 2011; Cohen and Jones 2011). Figure 3a, b show the seasonal-mean Z anomaly at 500 hPa during the two PDO phases. Only strong PDO years with a PDO index larger than 0.5 or smaller than −0.5 standard deviations are used. Significant anomalies of the opposite sign are observed over the North Pacific and northwestern Canada. Thus, PDO-related SST anomalies modify the tropospheric circulation downstream of the maximum SST anomalies. As shown later, these circulation anomalies influence vertically propagating planetary-scale waves during +PWSV and −PWSV events.

Figure 3c, d show the 500 hPa Z anomalies integrated over a lag of −11 to −1 days before the onset of +PWSV and −PWSV events, respectively. A large positive anomaly appears over northern Europe in both cases, which is somewhat expected because the positive Z anomaly over the Ural Mountains and northern Europe is a well-known precursor to WSV events (Garfinkel et al. 2010; Kolstad and Charlton-Perez 2011; Nishii et al. 2010; Cohen and Jones 2011). A comparison of the two cases, however, reveals a remarkable difference over the North Pacific. The negative anomaly appears during +PWSV events while the positive anomaly is evident during the opposite cases. The central location of these anomalies is close to that of seasonal-mean anomalies as shown in Fig. 3a, b, indicating that they partly reflect the mean flow response to the PDO.

Another notable difference between Fig. 3c, d is the spatial scale of the anomalies. During +PWSV events, the negative Z anomaly over the North Pacific is elongated in a broad region from East Asia to the west coast of the US. This contrasts to the pattern of −PWSV events, during which a negative anomaly is confined over East Asia and Northeast Russia, with a significant positive anomaly from Japan to Alaska. Thus, the zonal scale of the Z anomalies during +PWSV events is larger than that during −PWSV events. As discussed later, this scale has an important implication for the W1 and W2 activities in the course of

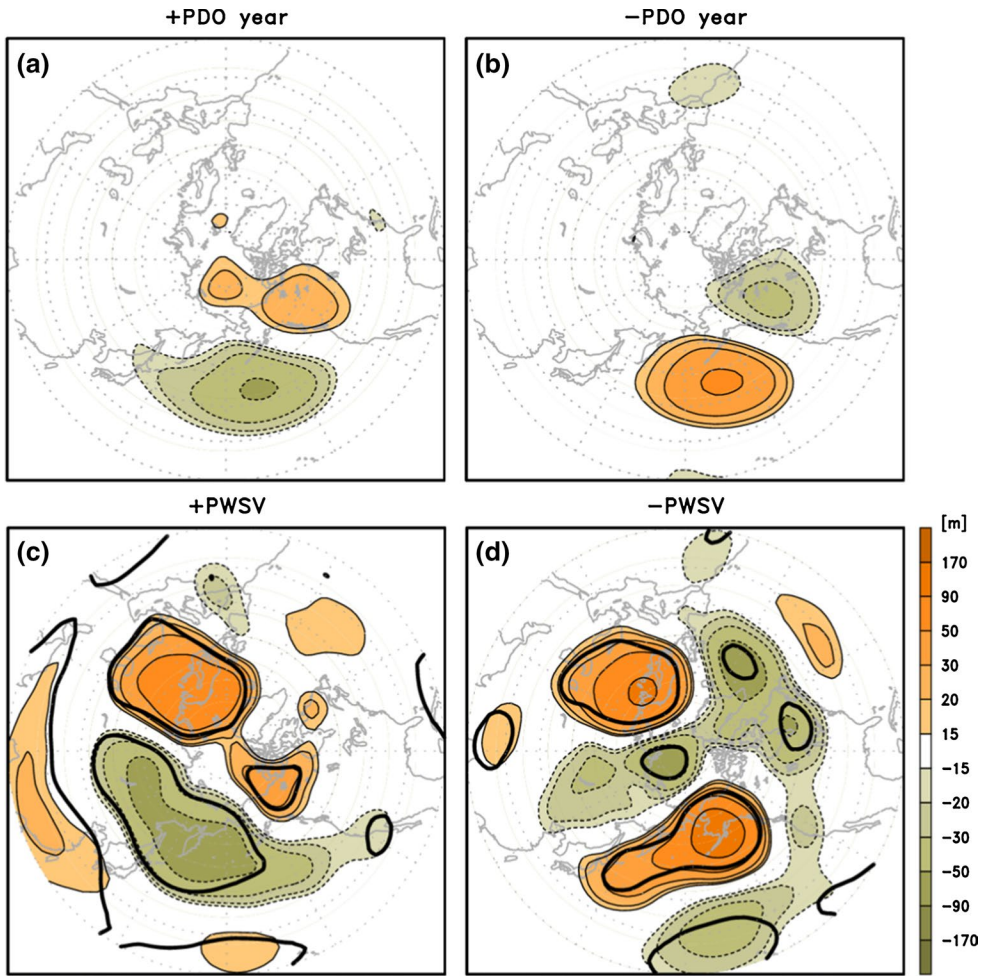

Fig. 3 Mean Z anomaly at 500 hPa for positive (**a**) and negative (**b**) PDO years. The Z anomalies at 500 hPa averaged from −11 to −1 days before the occurrence of +PWSV (**c**) and −PWSV (**d**). The area inside the *thick black lines* satisfies the 95 % confidence level

WSV events. Notably, the spatial pattern of the Z anomalies shown in Fig. 3c, d are likely to be qualitatively similar to the model results of Hurwitz et al. (2012; see their Fig. 8), where PDO-like SST anomalies chosen from the strongest events are prescribed in the AGCM. In fact, the authors noted that the SSWs in cold (warm) SSTs experiment have W1 (W2)-like structures. Therefore, the different preconditioning of WSV events during the two PDO phases is a robust dynamical feature that implies PDO-related SST anomalies are one of the key factors that influence the occurrence of WSV events.

3.2 Wave drivings during +PWSV and −PWSV events

To examine the planetary-scale wave activities that influence the occurrence of +PWSV and −PWSV events in the context of linear interference, we first examine the climatological W1 and W2 patterns in the 500-hPa geopotential height field. It is evident from Fig. 4a, b that the W1 component exhibits a negative anomaly from East Asia to the Northeast Pacific and a positive anomaly from North America to eastern Europe. By contrast, the W2 component has two positive anomaly centers: one over eastern Europe and the other along the west coast of North America, including Alaska. These wave patterns are compared with the W1 and W2 components of the preconditioning anomalies of the +PWSV and −PWSV events (Fig. 4c–f). In the case of +PWSV events (Fig. 4c, d), both the W1 and W2 components are in phase with the climatological patterns (comparing the top and middle rows). Therefore, both the W1 and W2 waves are enhanced during the onset of the +PWSV events, possibly strengthening wave forcing in the stratosphere. Note that the amplitude of the W1 component is slightly stronger than that of W2 component, indicating a stronger contribution of W1 than of W2 waves. In the case of −PWSV events (Fig. 4e, f), the W1 component tends to be out of phase with the climatological wave, whereas the W2 component is significantly strong and nearly in phase with the climatological wave (comparing the top and bottom rows). This result may suggest that −PWSV events are driven by the W2 wave driving despite the slight suppression of the W1 wave amplitude. Although not shown, similar results are found at 500 hPa and in the upper troposphere.

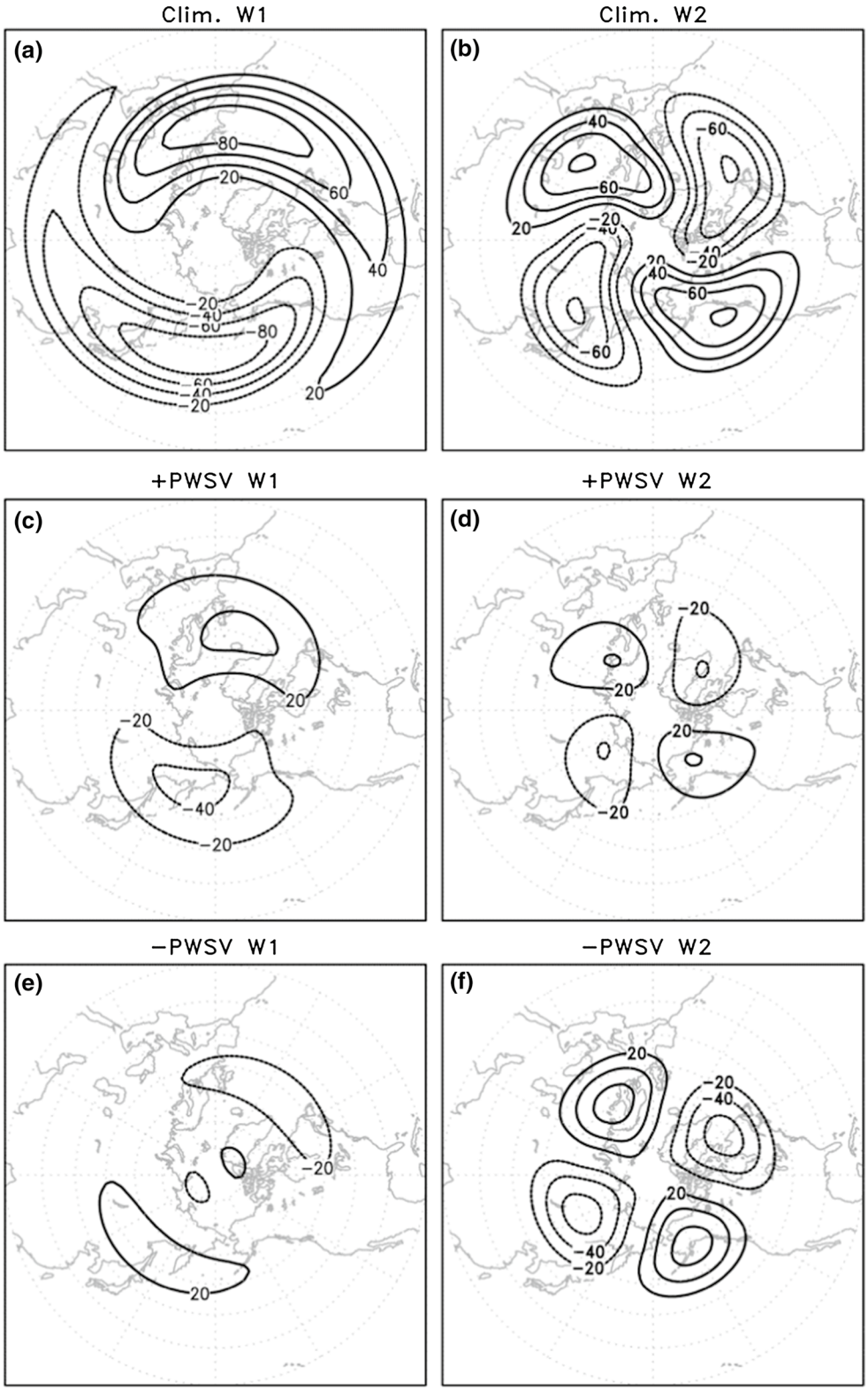

Fig. 4 Climatological planetary wavenumber-one (**a**) and wavenumber-two (**b**) patterns of the Northern Hemispheric circulation at 500-hPa during the boreal winter. Wavenumber-one (**c**) and wavenumber-two (**d**) patterns during preconditioning of the WSV occurrence in the positive PDO winter. **e**, **f** are the same as (**c**) and (**d**), respectively, except in the negative PDO winter

The above relationship is robustly observed in individual +PWSV and −PWSV events, as illustrated in Fig. 5, which shows the coefficients of the preconditioning anomalies projected onto the climatological wave pattern at 500 hPa. The positive values indicate that preconditioning anomalies of WSV events are in phase with the climatological pattern. During +PWSV events, W1 anomalies are positively projected onto the climatological W1 pattern. As

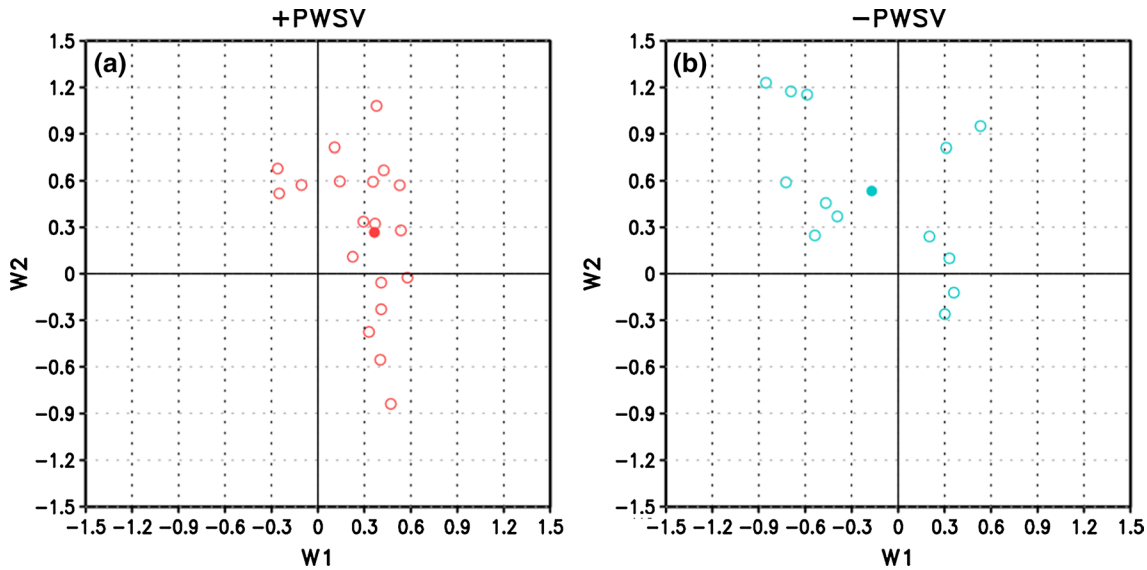

Fig. 5 Coefficients of the wave components of the preconditioning pattern of individual WSV events during positive (**a**) and negative (**b**) PDO winters projected onto the climatological patterns. The *filled circles* in **a**, **b** represent the ensemble mean of the projection coefficients in +PWSV and −PWSV events, respectively

expected from Fig. 4d, the majority of such events are also positively projected onto the climatological W2 pattern (Fig. 5a). During −PWSV events, all but two cases are positively projected onto the climatological W2 pattern. The W1 anomalies, however, are either positively or negatively projected onto the climatological waves.

It is important to note that linear interference does not necessarily represent wave activity in the upper troposphere and lower stratosphere. Therefore, we calculated the zonal-mean eddy heat flux averaged over 40°–70°N at 100 hPa, which is often used to quantify wave activity in the lower stratosphere (Polvani and Waugh 2004). Figure 6a shows the lag composites of the total eddy heat flux anomaly according to the PDO phases. There is essentially no difference in the evolution of the total eddy heat flux between +PWSV and −PWSV events. The same quantity, but for the sum of only the W1 and W2 components, is illustrated in Fig. 6b. The values are remarkably similar to those in Fig. 6a, indicating that the upward wave propagation in the lower stratosphere is predominantly controlled by the W1 and W2 components.

We next examine the relative importance of the W1 and W2 components during the +PWSV and −PWSV events (Fig. 7a, b). In the +PWSV events, the W1 component is most important (Fig. 7a). About 80 % of total eddy heat flux anomaly is explained by the W1 component during the preconditioning phase (lag of −11 to −1 days). Although the W2 component is also positive, its contribution to the total heat flux anomaly is much smaller than that of the W1 component. This result is consistent with the tropospheric preconditioning patterns shown in Fig. 4c, d. However, in

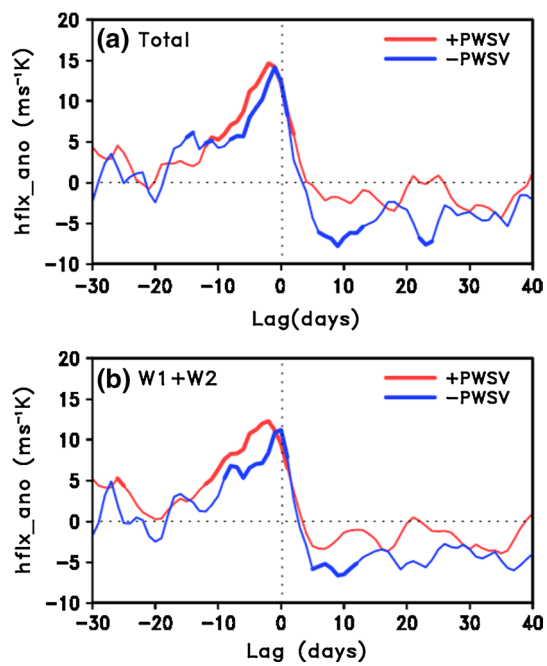

Fig. 6 **a** Lag composite of the meridional heat flux averaged over 40°–70°N at 100 hPa during WSV events in positive and negative PDO winters. **b** Same as (**a**) but for the sum of the wavenumber-one and wavenumber-two meridional heat fluxes. The *thick red* and *blue lines* represent the periods that satisfied the 95 % confidence level in each PDO phase

the case of the −PWSV events, there is almost no contribution from the W1 component (Fig. 7b), indicating that W1 does not contribute to the occurrence of WSV events

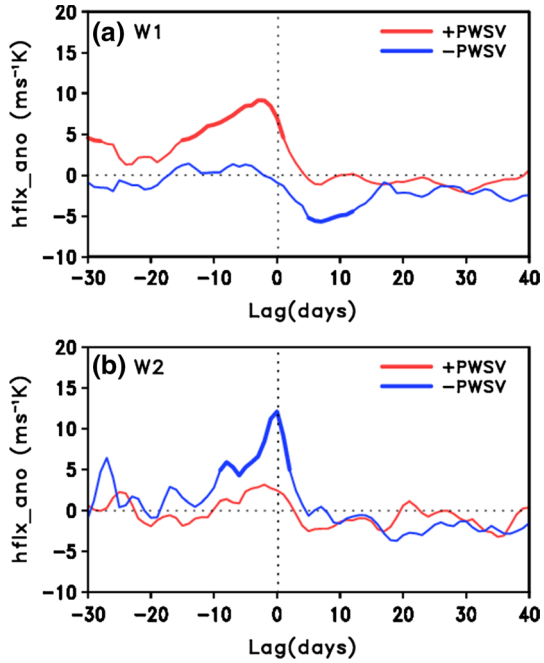

Fig. 7 **a** Lag composite of the wavenumber-one component of zonal-mean meridional heat flux averaged over 40°–70°N at 100 hPa during WSV events in positive and negative PDO winters. **b** Same as (**a**) but for the wavenumber-two component. The *thick red* and *blue lines* represent the periods that satisfied the 95 % confidence level in each PDO phase

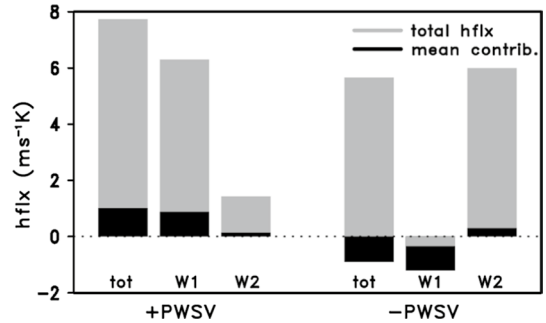

Fig. 8 Contributions of the mean circulation to the total and wavenumber components of the anomalous heat flux during the preconditioning of WSV events in positive and negative PDO winters

to a large extent; wave driving is instead controlled by the W2 component. These results clearly indicate that the wave drivings of WSV events are highly sensitive to the PDO phases. The +PWSV events are, to the first order, driven by W1 disturbances. By contrast, the −PWSV events are largely driven by W2 perturbations.

3.3 Contribution of PDO-induced mean circulation change to +PWSV and −PWSV events

What causes the difference in upward-propagating planetary-scale waves between the +PWSV and −PWSV events? To address this issue, comprehensive dynamical analyses are needed. In this section, we only examine the possible role of the mean flow change in response to the PDO. Figure 8 presents the total eddy heat flux anomaly integrated over a lag of −11 to −1 days from Fig. 7 (gray bars). The heat flux anomaly is further decomposed into the PDO-related mean component and into W1 and W2 components. Here, the PDO-related mean component (black bars in Fig. 8) is quantified by averaging the heat flux anomaly during the positive and negative PDO winters, regardless of WSV events. It is evident that the total eddy heat flux anomaly is not directly controlled by the mean flow change. During the positive PDO phase, the W1 component of the PDO-related mean circulation change contributes positively to the total eddy heat flux anomaly, implying that the PDO-related mean circulation change plays a non-negligible role in driving upward-propagating waves. However, the W1 contributes negatively during the negative PDO phase, potentially suppressing the occurrence of WSV events. As such, the PDO-related mean circulation change can partly explain the difference in the W1 anomalies between +PWSV and −PWSV events (see also Fig. 4c, e).

The W2 components of the PDO-related mean circulation changes project positively onto the total eddy heat flux anomaly in both events (Fig. 8). However, the W2 magnitudes are much weaker than those of the W1 components. This indicates a minimal role of the mean flow change in driving WSV events. Here, the weak-amplitude W2 component is caused by the geographical location of the W2 anomaly. The maximum W2 anomaly is located in high latitudes compared with the center of the PDO-related mean circulation over the North Pacific, as found in a comparison between Figs. 3b and 4f.

To further examine the impact of the PDO-related mean circulation change in driving WSV events, we removed the mean circulation anomaly from the preconditioning anomalies of +PWSV and −PWSV events. The resulting anomaly, which is basically the difference between the bottom and top panels of Fig. 3, is demonstrated in Fig. 9. A comparison of Fig. 9a with Fig. 3c reveals that the negative Z anomaly over the North Pacific, implying the enhancement of W1 component, is significantly reduced in the case of +PWSV events, whereas it does not change much in the case of −PWSV events, compared between Figs. 3d and 9b. These features also indicate that the PDO-related mean circulation changes mainly contribute to the +PWSV events.

It is important to state that the negligible contribution of the mean-flow anomaly to W2 driving in triggering the −PWSV events (e.g., Fig. 8b) does not imply that −PWSV

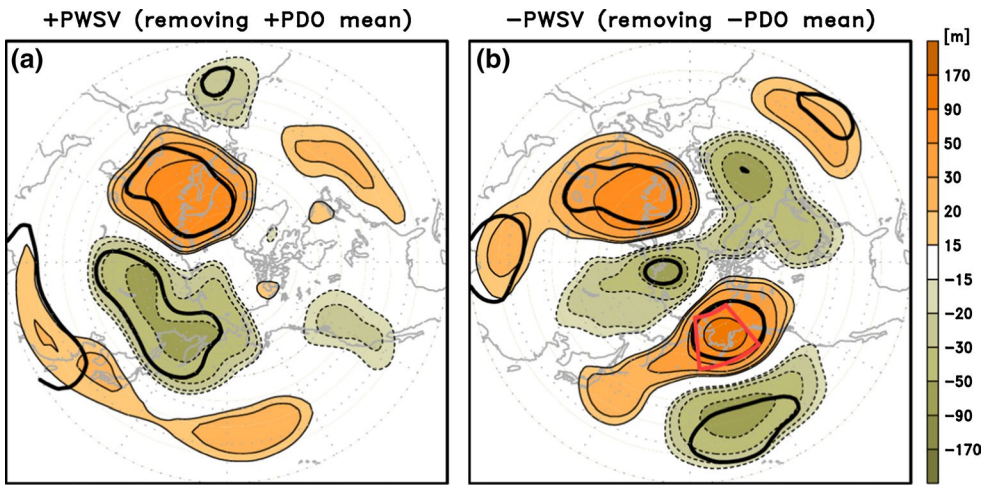

Fig. 9 Z anomaly patterns at 500 hPa that are removed from the mean circulation related to positive (**a**) and negative (**b**) PDO winters during preconditioning of the WSV occurrence. The *red box* in **b** represents the region defined as Alaska. The area inside the *thick black lines* satisfies the 95 % confidence level

events occur independently of the PDO phase. Instead, it should be interpreted that −PWSV events are driven by low-frequency eddies, which are modulated by the PDO rather than direct mean flow change. Likewise, although the mean flow change contribute partly to enhancement of W1 driving, +PWSV events are not simply driven by the mean flow change related to the PDO. Figure 8a suggests that the difference between the gray and black bars may be more important than the black bar itself.

3.4 Possible cause of predominant W2 driving in −PWSV events

In this section, we attempt to explain how the −PWSV events are triggered by the W2 component of planetary-scale waves. One of the main differences between Fig. 9a, b is the significant positive Z anomaly at high latitudes (50°–70°N) of the North Pacific centered over Alaska and the negative Z anomaly over the North Atlantic during −PWSV events (Fig. 9b). In terms of linear interference, this positive anomaly over Alaska and a negative anomaly over the North Atlantic play a crucial role in the enhancement of W2 activity during the −PWSV events (Fig. 4f). Therefore those nature need to be better understood. At first, the negative Z anomaly over the North Atlantic in the −PWSV events, which is not directly related to the PDO-induced mean circulation change, may result from Atlantic SST variability. Recent studies have shown the out-of-phase relationship between the PDO and Atlantic Multi-decadal Oscillation (AMO) in recent decades (McCabe et al. 2004). However, no evidence has been found (not shown).

To examine the possible cause of strong positive Z anomalies over Alaska during the −PWSV events, we investigated the low-frequency variability between the two PDO phases (not shown). Here, low-frequency variability is defined as the variance of the 500 hPa Z anomalies that are filtered with 11-day moving average. Similar to the mean flow response (Fig. 3a, b), significant differences are observed over the Bering Sea and Alaska. Specifically, the local variability over the Alaska is stronger during the negative PDO winters (103.4 m) than during the positive winters (85.6 m). The difference between variabilities in two PDO winters is statistically significant. Although this difference may indicate that both the positive and negative anomalies are enhanced during the negative PDO winters (i.e., broadening of the probability density function), the probability density function of the Z anomalies over Alaska (averaged over the red box in Fig. 9a), one of precursor regions of WSV events (Garfinkel et al. 2010), shows a slight shift toward positive Z anomalies; extremely positive Z anomalies substantially increase (Fig. 10a). A more frequent occurrence of strong positive Z anomalies likely provides preferable conditions that increase the chance of upward-propagating W2, as discussed in the context of linear interference.

How is the low-frequency variability over Alaska enhanced during negative PDO winters? The variability is likely related to the mean flow changes associated with the PDO. Figure 10b shows the difference in the seasonal-mean zonal wind at 300 hPa between the positive and negative PDO winters. A dipole pattern is observed over the North Pacific. This feature indicates a northeastward shift and slight weakening of the Pacific jet during the negative PDO phase compared with the climatological mean. This feature results in diffluent flow in the high latitudes of the Northeast Pacific (Shutts 1983; Colucci 2001), providing preferable conditions for low-frequency eddy activities, such as blocking. Several studies noted more frequent blocking over the North Pacific, including the northeastern Pacific, when the Pacific jet shifts poleward during cold ENSO winters (Renwick and Wallace 1996; Chen and Dool 1997; Compo et al. 2001; Dunn-Sigouin and Son 2013; Barrippedro and Calvo 2014). Strong low-frequency eddy activity can also be related to the enhanced transient eddy

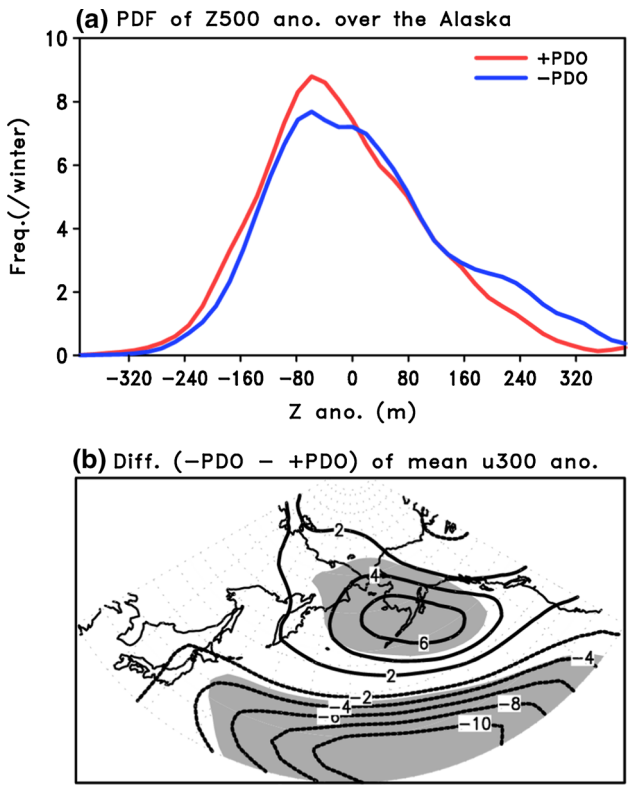

Fig. 10 **a** Probability density functions of the Z anomaly at 500 hPa, stratified by the PDO phases. **b** Difference map of the zonal wind at 300 hPa between the positive and negative PDO winters. The *gray shading* in **b** represents the area that satisfied the 95 % confidence level

feedback. In general, the poleward shift of the Pacific jet accompanies the poleward shift of storm-track (Renwick and Wallace 1996; Chen and Dool 1997). The changes in storm-track eddies can enhance low-frequency eddy activities in high latitudes, as discussed in Lau (1988), Jin et al. (2006a, b), and Kug and Jin (2009). Although more quantitative analyses are needed, the predominant contribution of W2 in driving −PWSV events likely results from the northeastward shift of the Pacific jet and from the associated synoptic eddy feedback to low-frequency eddies over the Northeast Pacific, including Alaska.

4 Conclusions and discussion

This study explores the possible impacts of the PDO on the frequency and morphology of WSV events in the Northern Hemisphere winter. WSV events during positive PDO years (+PWSV events) are more frequent than those during negative PDO years (−PWSV events). This difference in frequency is statistically significant, although the exact reason remains to be determined. Additionally, the tropospheric wave drivings of +PWSV events are very different from those of −PWSV events. In general, the former wave drivings are dominated by W1 disturbances, whereas the latter are controlled by W2 disturbances. These features are robustly found in the eddy heat flux anomalies at 100 hPa. In terms of dynamical processes, the main contribution of W1 to +PWSV events is partly caused by the PDO-induced mean-flow change, and the contribution of W2 to −PWSV events is not directly related to the mean flow change. The enhancement of W2 wave driving in −PWSV events is likely to be indirectly affected by the PDO through anomalous low-frequency eddy activities.

Recent studies have shown that North Pacific SST anomalies can influence both the tropospheric (Frankignoul and Sennechael 2007; Taguchi et al. 2012; Lee et al. 2012) and stratospheric circulations (Jadin et al. 2010; Hurwitz et al. 2012) on interannual to decadal timescales. By integrating AGCM with North Pacific SST anomalies, Hurwitz et al. (2012) found that North Pacific SSTs can modulate the frequency of WVS (SSW in their definition) events in a major way. Specifically, more frequent WVS events occur in the presence of anomalously cold North Pacific SSTs. More importantly, such events are typically preceded by W1 disturbances in the troposphere. Given that North Pacific SSTs are anomalously cold during positive PDO phases, these results are very consistent with the main conclusions of the present study. In this regards, this study provides observational evidence of the PDO-related stratospheric variability, complementing the modeling study of Hurwitz et al. (2012). Although Hurwitz et al. (2012) prescribed chosen from the strongest events strong SST anomalies in their model simulations to identify extratropical SST-induced WSV events, it is noteworthy that SST-induced circulation over the North Pacific can modulate the planetary-scale waves that potentially influence the occurrences of WSV events.

The PDO has a strong inter-annual variability, in addition to long-term decadal fluctuations. Such variability on an interannual time scale is somewhat related to the El Nino-Southern Oscillation (ENSO). To separate the PDO (or extratropical SST anomalies) from the ENSO (or tropical SST anomalies), the same analyses are repeated by excluding strong ENSO years. Although composite fields are less significant due to the reduced sample size, qualitatively similar results are found.

In this study, the nature of low-frequency eddies that drive W1 and W2 disturbances during the precondition of WSV events (the difference between the gray and black bars in Fig. 8) is not examined in detail. Such eddies are particularly important in driving −PWSV events, as shown in Fig. 8. The low-frequency eddies could be related to blocking, as discussed by Barrippedro and Calvo (2014) that note differences in the blocking precursor of SSW according to ENSO phases, but require further investigation.

Nevertheless, because factors such as the PDO are slowly varying components of the climate system beyond the intra-seasonal time scale, the results of the connection between WSV occurrence and PDO-related circulations will be useful for seasonal predictions based on the variability of the stratospheric polar vortex.

Acknowledgments This work was supported by National Research Foundation (NRF-2014R1A2A2A01003827). SWS is partly supported by Korea Ministry of Environment as "Climate Change Correspondence Program". MKS is supported by KOPRI (PE15010).

References

Andrews DG, Holton JR, Leovy CB (1987) Middle atmosphere dynamics. Academic Press, London, p 489

Baldwin MP, Dunkerton TJ (1999) Downward propagation of the Arctic Oscillation from the stratosphere to the troposphere. J Geophys Res 104:30937–30946

Baldwin MP, Dunkerton TJ (2001) Stratospheric harbingers of anomalous weather regimes. Science 294:581–584. doi:10.1126/science.1063315

Baldwin MP, Thompson DW (2009) A critical comparison of stratosphere–troposphere coupling indices. Q J R Mereorol Soc 135:1661–1672. doi:10.1002/qj.479

Barrippedro D, Calvo N (2014) On the relationship between ENSO, stratospheric sudden warming, and blocking. J Clim 27:4704–4720

Bell CJ, Gray LJ, Charlton-Perez AJ, Joshi MM, Scaife AA (2009) Stratospheric communication of El Nino teleconnections to European winter. J Clim 22:4083–4096. doi:10.1175/2009JCLI2717.1

Black RX (2002) Stratospheric forcing of surface climate in the Arctic oscillation. J Clim 15:268–277

Bronnimann S (2007) Impact of El Nino-Southern Oscillation on European climate. Rev Geophys 45:RG3003. doi:10.1029/2006RG000199

Butler AH, Polvani LM (2011) El Niño, La Niña, and stratospheric sudden warmings: a reevaluation in light of the observational record. Geophys Res Lett 38:L13807. doi:10.1029/2011GL048084

Butler A, Seidel D, Hardiman S, Butchart N, Birner T, Match A (2015) Defining sudden stratospheric warmings. Bull Am Meteor Soc. doi:10.1175/BAMS-D-13-00173.1

Charlton AJ, Polvani LM, Perlwitz J, Sassi F, Manzini E, Shibata K, Pawson S, Nielsen JE, Rind D (2007) A new look at stratospheric sudden warmings. Part II: evaluation of numerical model simulations. J Clim 20:470–488

Charron M, Polavarapu S, Buehner M, Vaillancourt PA, Charette C, Roch M, Morneau J, Garand L, Aparicio JM, MacPherson S, Pellerin S, StJames J, Heilliette S (2012) The stratospheric extension of the Canadian global deterministic medium-range weather forecasting system and its impact on tropospheric forecasts. Mon Weather Rev 140:1924–1944

Chen WY, Dool HM (1997) Asymmetric impact of tropical SST anomalies on atmospheric internal variability over the North Pacific. J Atmos Sci 54:725–740

Cohen J, Jones J (2011) Tropospheric precursors and stratospheric warmings. J Clim 25:1779–1790

Cohen J, Salstein D, Saito K (2002) A dynamical framework to understand and predict the major Northern Hemisphere mode. Geophys Res Lett 29(10):1412. doi:10.1029/2001GL014117

Colucci SJ (2001) Planetary-scale preconditioning for the onset of blocking. J Atmos Sci 58:933–942

Compo GP, Sardeshmukh PD, Penland C (2001) Change of subseasonal variability associated with El Nino. J Clim 14:3356–3373

Dunn-Sigouin E, Son SW (2013) Northern Hemisphere blocking frequency and duration in the CMIP5 models. J Geophys Res 118:1179–1188

Frankignoul C, Sennechael N (2007) Observed influence of North Pacific SST anomalies on the atmospheric circulation. J Clim 20:592–606

Free M, Seidel DJ (2009) Observed El Niño-Southern Oscillation temperature signal in the stratosphere. J Geophys Res 114:D23108. doi:10.1029/2009JD012420

Garfinkel CI, Hartmann DL (2007) Effects of the El Nino-Southern Oscillation and the quasi-biennial oscillation on polar temperatures in the stratosphere. J Geophys Res 112:D19112. doi:10.1029/2007JD008481

Garfinkel CI, Hartmann DL, Sassi F (2010) Tropospheric precursors of anomalous Northern Hemisphere stratospheric polar vortices. J Clim 23:3282–3299. doi:10.1175/2010JCLI3010.1

Garfinkel CI, Butler AH, Waugh DW, Hurwitz MM, Polvani LM (2012) Why might stratospheric sudden warmings occur with similar frequency in El Nino and La Nina winters? J Geophys Res Atmos 117:D19106. doi:10.1029/2012JD017777

Gerber EP et al (2012) Assessing and understanding the impact of stratospheric dynamics and variability on the earth system. Bull Am Meteorol Soc 93:845–859. doi:10.1175/BAMS-D-11-00145.1

Hartley DE, Villarin J, Black RX, Davis CA (1998) A new perspective on the dynamical link between the stratosphere and troposphere. Nature 391:471–474

Hurwitz MM, Newman PA, Garfinkel CI (2012) On the influence of North Pacific sea surface temperature on the Arctic winter climate. J Geophys Res 117:D19110. doi:10.1029/2012JD017819

Jadin EA, Wei R, Zyalyaeva YA, Wen Chen, Wang L (2010) Stratospheric wave activity and the Pacific Decadal Oscillation. J Atmos Solar Terr Phys 72:1163–1170. doi:10.1016/j.jastp.2010.07.009

Jin FF, Pan LL, Watanabe M (2006a) Dynamics of synoptic eddy and low-frequency flow interaction, Part I: a linear closure. J Atmos Sci 63:1677–1694

Jin FF, Pan LL, Watanabe M (2006b) Dynamics of synoptic eddy and low-frequency flow interaction, Part II: a theory for low-frequency modes. J Atmos Sci 63:1695–1708

Kalnay E, Kanamitsu M, Kistler R, Collins W, Deaven D, Gandin L, Iredell M, Saha S, White G, Woollen J, Zhu Y, Chelliah M, Ebisuzaki W, Higgins W, Janowiak J, Mo KC, Ropelewski C, Wang J, Leetmaa A, Reynolds R, Jenne R, Joseph D (1996) The NCEP/NCAR 40-year reanalysis project. Bull Am Meteorol Soc 77:437–471

Kim JY, Chun HY, Kang MJ (2014) Changes in the Brewer–Dobson circulation for 1980–2009 rvealed in MERRA reanalysis data. Asia Pac J Atmos Sci 50(1):625–644

Kolstad EW, Charlton-Perez AJ (2011) Observed and simulated precursors of stratospheric polar vortex anomalies in the Northern Hemisphere. Clim Dyn 37:1443–1456. doi:10.1007/s00382-010-0919-7

Kolstad EW, Breiteig T, Scaife AA (2010) The association between stratospheric weak polar vortex events and cold air outbreaks in the Northern Hemisphere. Q J R Meteorol Soc 136:886–893. doi:10.1002/qj.620

Kug JS, Jin FF (2009) Left-hand rule for synoptic eddy feedback on low-frequency flow. Geophys Res Lett 36:L05709. doi:10.1029/2008GL036435

Lau NC (1988) Variability of the observed midlatitude storm tracks in relation to low-frequency changes in the circulation pattern. J Atmos Sci 45:2718–2743

Lee YY, Kug JS, Lim GH, Watanabe M (2012) Eastward shift of the Pacific/North American pattern on an interdecadal time scale and associated synoptic eddy feedback. Int J Climatol 32:1128–1134

Limpasuvan V, Thompson DWJ, Hartmann DL (2004) The life cycle of the northern hemisphere sudden stratospheric warmings. J Clim 17:2584–2596

Manzini EM, Giorgetta A, Kornbluth L, Roeckner E (2006) The influence of sea surface temperatures on the northern winter stratosphere: ensemble simulations with the MAECHAM5 model. J Clim 19:3863–3881

Martineau P, Son SW (2013) Planetary-scale wave activity as a source of varying tropospheric response to stratospheric sudden warming events: a case study. J Geophys Res 118:10994–11006

Martius O, Polvani LM, Davies HC (2009) Blocking precursors to stratospheric sudden warming events. Geophys Res Lett 36:L14806. doi:10.1029/2009GL038776

Matsuno T (1970) Vertical propagation of stationary planetary waves in the winter Northern Hemisphere. J Atmos Sci 27:871–883

Matsuno T (1971) A dynamical model of stratospheric warmings. J Atmos Sci 28:1479–1494

McCabe GJ, Palecki MA, Betancourt JL (2004) Pacific and Atlantic Ocean influences on multidecadal drought frequency in the United States. Proc Natl Acad Sci 101:4136–4141

Mitchell DM, Gray LJ, Anstey J, Baldwin MP, Charlton-Perez AJ (2013) The influence of stratospheric vortex displacements and splits on surface climate. J Clim 26:2668–2682

Nishii K, Nakamura H, Miyasaka T (2009) Modulations in the planetary wave field induced by upward propagating Rossby wave packets prior to stratospheric sudden warming events: a case-study. Q J R Meteorol Soc 135(638):39–52. doi:10.1002/qj.359

Nishii K, Nakamura H, Orsolini YJ (2010) Cooling of the wintertime Arctic stratosphere induced by the western Pacific teleconnection pattern. Geophys Res Lett 37:L13805. doi:10.1029/2010GL043551

Perlwitz J, Harnik N (2004) Downward coupling between the stratosphere and troposphere: the relative roles of wave and zonal mean processes. J Clim 17:4902–4909

Polvani LM, Waugh DW (2004) Upward wave activity flux as a precursor to extreme stratospheric events and subsequent anomalous surface weather regimes. J Clim 17:3548–3554

Renwick JA, Wallace JM (1996) Relationships between North Pacific winter time blocking, El Nino and the PNA pattern. Mon Weather Rev 124:2071–2076

Sassi F, Kinnison D, Bolville BA, Garcia RR, Roble R (2004) Effect of El-Nino Southern Oscillation on the dynamical, thermal, and chemical structure of the middle atmosphere. J Geophys Res 109:D17108. doi:10.1029/2003JD004434

Shutts GJ (1983) The propagation of eddies in diffluent jetstreams: eddy vorticity forcing of 'blocking' flow fields. Q J R Meteorol Soc 109:737–761

Sigmond M, Scinocca JF, Kharin VV, Shepherd TG (2013) Enhanced seasonal forecast skill following stratospheric sudden warmings. Nat Geosci 6:98–102

Smith KL, Fletcher CG, Kushner PJ (2010) The role of linear interference in the annular mode response to extratropical surface forcing. J Clim 23:6036–6050. doi:10.1175/2010JCLI3606.1

Stan C, Straus DM (2009) Stratospheric predictability and sudden stratospheric warming events. J Geophys Res 114:D12103. doi:10.1029/2008JD011277

Taguchi M, Hartmann DL (2006) Increased occurrence of stratospheric sudden warming during El Nino as simulated by WAACM. J Clim 19(324):332. doi:10.1175/JCLI3655.1

Taguchi B, Nakamura H, Nonaka M, Komori N, Kuwano-Yoshida A, Takaya K, Goto A (2012) Seasonal evolutions of atmospheric response to decadal SST anomalies in the North Pacific subarctic frontal zone: observations and a coupled model simulation. J Clim 25:111–139

Thompson DWJ, Baldwin MP, Wallace JM (2002) Stratospheric connection to Northern Hemisphere wintertime weather: implications for prediction. J Clim 15:1421–1428

Tripathi O, Baldwin M, Charlton-Perez A, Charron M, Eckermann S, Gerber E, Harrison RG, Jackson DR, Kim BM, Kuroda Y, Lang A, Lee C, Mahmood S, Mizuta R, Roff G, Sigmond M, Son SW (2014) The predictability of the extra-tropical stratosphere on monthly timescales and its impacts on the skill of tropospheric forecasts. Q J R Meteorol Soc. doi:10.1002/qj.2432

Yun KS, Seo YW, Ha KJ, Lee JY, Kajikawa Y (2014) Interdecadal changes in the Asian winter monsoon variability and its relationship with ENSO and AO. Asia Pac J Atmos Sci 50(4):531–540